

Apolipoprotein A-I structural organization in high-density lipoproteins isolated from human plasma

Rong Huang¹, R A Gangani D Silva¹, W Gray Jerome², Anatol Kontush³⁻⁵, M John Chapman³⁻⁵, Linda K Curtiss⁶, Timothy J Hodges⁷ & W Sean Davidson¹

High-density lipoproteins (HDLs) mediate cholesterol transport and protection from cardiovascular disease. Although synthetic HDLs have been studied for 30 years, the structures of human plasma-derived HDL and its major protein apolipoprotein apoA-I are unknown. We separated normal human HDL into five density subfractions and then further isolated those containing predominantly apoA-I (LpA-I). Using cross-linking chemistry and mass spectrometry, we found that apoA-I adopts a structural framework in these particles that closely mirrors that in synthetic HDL. We adapted established structures for synthetic HDL to generate the first detailed models of authentic human plasma HDL in which apoA-I adopts a symmetrical cage-like structure. The models suggest that HDL particle size is modulated by means of a twisting motion of the resident apoA-I molecules. This understanding offers insights into how apoA-I structure modulates HDL function and its interactions with other apolipoproteins.

The inverse correlation between plasma HDL cholesterol levels and the risk for cardiovascular disease is well established¹. As its most abundant protein, apoA-I mediates many HDL functions. It is a key player in the HDL-mediated process of reverse cholesterol transport, and it shows cardioprotective anti-inflammatory and antioxidative properties². Unfortunately, the conformational plasticity of apoA-I combined with HDL's staggering compositional heterogeneity has precluded an understanding of how apoA-I structure mediates these critical functions.

Most structural studies of apoA-I in HDL have used reconstituted particles (rHDL) that mimic *in vivo* intermediates between lipid-free apoA-I and mature spherical HDL (reviewed in refs. 3,4). Recent work on these phospholipid-containing discoidal particles suggests that apoA-I molecules adopt a 'double-belt' orientation in which two apoA-I molecules wrap around a patch of phospholipid bilayer in an antiparallel fashion. They maintain a registry, stabilized by intermolecular salt bridges, in which the fifth amphipathic helix of each molecule overlaps^{5,6}. The basic tenets of this model have been supported by numerous experimental studies⁷⁻¹⁰, though several variations on the model have been proposed. Given such colorful names as the 'belt-buckle'^{7,11}, the 'looped belt'¹² and 'solar flares'¹³, these propose localized conformational features that may be of key importance to apoA-I interaction with plasma enzymes or exposure to oxidants. Another model¹⁴ postulates an elongated phospholipid micelle instead of a bilayer, though two recent molecular dynamics simulations have questioned the stability of such an

arrangement^{15,16}. Nevertheless, all these models maintain the basic intermolecular interactions of the 5/5 double belt.

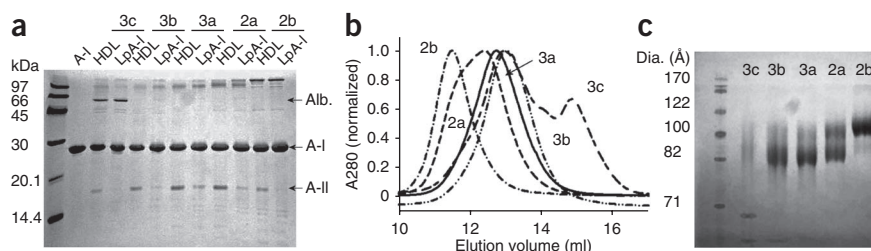
Unlike reconstituted discoidal particles, most circulating HDL contains a cholesteryl-ester- and triglyceride-rich core that results in a spherical shape. Instead of a bilayer, spherical HDLs show a highly curved phospholipid monolayer stabilized by surface apolipoproteins. Despite the differences in lipid structure, some have suggested that apoA-I conformations are related in both types of particles^{17,18}, whereas others point out differences in fluorescence emission, charge or proteolytic sensitivity^{19,20}. Recently, our laboratory addressed apoA-I structure in spherical particles by applying chemical cross-linking and mass spectrometry to both discoidal and spherical reconstituted HDL particles. We found apoA-I cross-linking patterns that strongly supported the 5/5 double-belt model in the discs, though a minor subset were consistent with a shifted 5/2 registry¹⁰. The cross-linking patterns in reconstituted spheres were highly similar to those in the discs, regardless of whether they contained three molecules of apoA-I in each particle or only two²¹.

How can three apoA-I molecules in spherical HDL adopt the same intermolecular contacts as only two in the discs? After considering numerous possibilities, we proposed a modification of the double-belt model called the trefoil model²¹. This invokes a bending of the planar belts and the intercalation of a similarly bent third apoA-I molecule so that all three adopt intermolecular contacts identical to the two in the discs. The resulting cage-like structure can stabilize surface phospholipids and contain the neutral lipid core and offers a parsimonious

¹Department of Pathology and Laboratory Medicine, University of Cincinnati, Cincinnati, Ohio, USA. ²Department of Pathology, Vanderbilt University Medical Center, Nashville, Tennessee, USA. ³Université Pierre et Marie Curie-Paris 6, Paris, France. ⁴National Institute of Health and Medical Research, Dyslipoproteinemia and Atherosclerosis Research Unit, Paris, France. ⁵Assistance Publique-Hopitaux de Paris, Groupe hospitalier Pitié-Salpêtrière, Paris, France. ⁶Department of Immunology and Vascular Biology, The Scripps Research Institute, La Jolla, California, USA. ⁷Department of Mathematical Sciences, University of Cincinnati, Cincinnati, Ohio, USA. Correspondence should be addressed to W.S.D. (Sean.Davidson@UC.edu).

Received 30 June 2010; accepted 15 December 2010; published online 13 March 2011; doi:10.1038/nsmb.2028

Figure 1 Isolation and characterization of human plasma LpA-I HDL particles. **(a)** An 18% SDS-PAGE analysis of the density-isolated HDL particles before (denoted as HDL_{2b-3c}) and after (denoted as LpA-I_{2b-3c}) sulfhydryl covalent chromatography. Lipid-free apoA-I is shown in lane 2 as a reference. Alb., albumin. **(b)** The indicated LpA-I subfractions were analyzed on a calibrated Superdex 200 gel-filtration column. The figure shows a representative result from three analyses of three independently prepared samples. **(c)** An 8–25% native PAGE analysis of BS³ cross-linked LpA-I subfractions. See **Table 1** for calculated diameters from panels **b** and **c**. All gels were stained with Coomassie blue.



solution to the similarity of the cross-links between rHDL discs and spheres. ApoA-I thus adopts a common structural framework regardless of particle shape, at least in reconstituted HDL.

Although the use of reconstituted particles for structural studies has been repeatedly validated by functional studies, the ultimate goal is to understand the authentic particles in circulation. However, inherent sample heterogeneity has precluded systematic studies of apoA-I structure in human plasma-derived HDL. Here, we took advantage of the fact that the cross-linking–mass spectrometry approach is not limited by the requirement of a homogeneous sample. We found that apoA-I adopts intermolecular interactions in plasma HDL that are very similar to those of the double-belt and trefoil models derived in reconstituted systems. Furthermore, our analysis supports assertions from molecular dynamics studies^{22,23} that apoA-I can twist across the particle surface to accommodate a range of HDL particle diameters. The resulting models are the first to describe apoA-I on authentic plasma HDL particles in detail.

RESULTS

HDL isolation

To study apoA-I in isolated human HDL, we used a one-step gradient ultracentrifugation method to obtain five density subfractions from normal human plasma that have been extensively characterized previously²⁴ (defined here as HDL_{2b}–HDL_{3c}). ApoA-I comprises between 60–70% of the total protein in HDL, with apoA-II the second most abundant at about 20%. Although the cross-linking technique can provide structural information in complex systems, we felt it was important to simplify the HDL particles as much as possible. Therefore, for each HDL density subfraction, we further isolated particles containing apoA-I but not apoA-II (LpA-I) using sulfhydryl covalent chromatography²⁵. Briefly, reduced HDL was passed down a sulfhydryl resin. The free disulfides at Cys6 in human apoA-II interact with the column to retain any particle containing apoA-II (or other disulfide-containing proteins; for example, apoJ) whereas particles not containing cysteine pass through. The products, defined as LpA-I_{2a}, LpA-I_{2b}, LpA-I_{3a}, LpA-I_{3b} and LpA-I_{3c}, were analyzed by SDS-PAGE (**Fig. 1a**). The apoA-II content of the LpA-I fractions was reduced by 70–80% compared to the original HDL sample. The separation was most effective in the HDL_{3c}, HDL_{3b} and HDL_{2b} fractions but moderately less so in the HDL_{3a} and HDL_{2a} fractions, in which we typically find the most apoA-II²⁶. Nevertheless, apoA-I represented some 80–90% of the Coomassie-stainable protein in the LpA-I particles. We recognize that these particles also contained trace levels of other proteins, the majority of which likely include the apoCs^{27,28}.

Once the LpA-I particles were separated, we measured their sizes on a calibrated gel filtration column (**Fig. 1b**) and by native gel electrophoresis (**Fig. 1c**). The diameter estimates from both techniques were consistent and ranged from 11.2 to 8.8 nm (**Table 1**). Native PAGE

indicated that the LpA-I_{2a} fraction contained two major populations, consistent with the non-Gaussian peak shape obtained by gel filtration. The LpA-I particle diameters were similar to those in the corresponding HDL particles, although the HDL particles showed evidence of at least two populations in all subfractions, consistent with the presence of apoA-II-containing particles (**Supplementary Fig. 1a**). Negative-stain EM showed that all particles were spheres and confirmed the size trends shown in **Figure 1** (**Supplementary Fig. 1b**). However, the measured EM diameters were notably smaller than those from gel filtration and native PAGE. This could be due to difficulties in resolving particle edges at this size (W.G.J., Vanderbilt University Medical Center, personal communication) or to deformation of particles during drying²³. Given that gel filtration and native PAGE offer hydrated diameters that are likely more physiologically relevant than EM, we averaged the diameters from these two techniques for the model building described below. Some albumin contamination was apparent in the LpA-I_{3c} fraction (**Fig. 1a**) as a shoulder eluting at 15 ml in the gel-filtration trace (**Fig. 1b**) and as a separate band in the native gel (**Fig. 1c**). The latter result suggests that albumin is probably not associated with the HDL particles.

LpA-I compositional analysis

We next characterized the particle chemical compositions (**Table 1**). The predicted particle densities, calculated from the weight percentages of the various components, correlated tightly with experimentally determined particle densities (**Supplementary Fig. 2**). To estimate the average number of apoA-I molecules per particle, we cross-linked the samples with the soluble homobifunctional cross-linker BS³. **Supplementary Figure 3** compares the susceptibility of LpA-I_{3a}, LpA-I_{2b} and a control reconstituted discoidal particle to cross-linking as a function of increasing cross-linker-to-protein ratio. All particles responded identically to the cross-linker, indicating that the extent of intermolecular contacts were similar between all three particles. The cross-linked LpA-I particles were analyzed by SDS-PAGE (**Fig. 2a**). All subfractions generated a diffuse band that decreased in size only slightly between LpA-I_{2b} and LpA-I_{3c}. The diffuse bands are typical of cross-linked proteins, because the reagent adds variable masses and the point(s) at which cross-linking occurs can affect migration on SDS gels¹¹. By measuring the smallest and largest band boundaries, we estimated that LpA-I_{2b} contains 5–7 molecules of apoA-I, whereas LpA-I_{2a} through LpA-I_{3c} contain 4–6, 4–6, 3–5 and 3–5 apoA-I molecules, respectively.

Before building structural models, it is critical to determine the average molar stoichiometry of protein and lipid components within each species. Knowing the molar ratio of each lipid component with respect to apoA-I (calculated from **Table 1**), we summed the partial specific volumes for each component to derive a predicted diameter for each particle (see Online Methods). This was calculated for

Table 1 Experimental characterization of LpA-I density subfractions

Particle	Density ^a (g ml ⁻¹)	GF diam. (Å) ^b	PAGE diam. (Å) ^c	Avg. diam. (Å)	aa (%) ^d	PL (%)	CE (%)	TG (%)	FC (%)
LpA-I _{2b}	1.09 ± 0.01	114 ± 3	110 ± 1	112	34.7	32.5	23.0	4.7	5.1
LpA-I _{2a}	1.11 ± 0.01	101 ± 8	95 ± 1	98	41.3	29.5	20.9	4.7	3.6
LpA-I _{3a}	1.14 ± 0.01	90 ± 3	90 ± 3	90	49.3	25.6	17.5	4.7	2.8
LpA-I _{3b}	1.16 ± 0.01	88 ± 2	89 ± 3	88	56.0	21.9	15.4	4.4	2.3
LpA-I _{3c}	1.19 ± 0.01	88 ± 2	88 ± 4	88	65.5	16.8	11.7	4.1	1.9

^aMeasured after the density gradient (mass/volume) from three independent preparations ± 1 s.d. aa, amino acid; PL, phospholipid; CE, cholesteryl ester; TG, triglyceride; FC, free cholesterol. ^bDetermined by relative elution volume on a Superdex 200 gel-filtration column calibrated with high molecular weight (HMW) standards (GE Healthcare) from three independent preparations ± 1 s.d. ^cDetermined by native PAGE against HMW standards (GE Healthcare) from three runs on one particle preparation ± 1 s.d. ^dThe LpA-I_{3c} fractions contained a detectable level of contaminating albumin (apparent in Fig. 1). To minimize artifacts in our composition calculations due to albumin contamination, we estimated the approximate ratio of albumin to all other proteins by densitometry and corrected our protein concentration values by this factor. Compositional data were obtained from two independent experiments and averaged. All percentages are w/w.

various numbers of apoA-I molecules per particle and then compared to the experimentally measured hydrodynamic diameter averaged from native PAGE and gel filtration (Table 1). A sample calculation is shown in Figure 2b for the LpA-I_{2b} particle. As the putative number of apoA-I molecules was increased, the predicted volume (and hence diameter) of the particle increased. At five apoA-I molecules per particle, the theoretical diameter matched closely with the experimentally determined diameter for LpA-I_{2b} (Fig. 2b, dotted line). This also fell within the range of expected apoA-I molecules determined by cross-linking (Fig. 2b, bracket). When we made this calculation for all LpA-I particles, we were surprised to find that LpA-I_{2a-3c} all averaged four molecules per particle. The concordance between calculated and experimental particle diameters is shown in Supplementary Figure 4. This suggests that a transition from a diameter of 11.2 nm to 9.8 nm involves the loss of one molecule of apoA-I, on average. However, changes in diameter from 9.8 nm to 8.8 nm can all be accommodated with four molecules remaining on the particle. These determinations represent averages for each subfraction and do not preclude the possibility that the LpA-I_{3c} fraction, for example, contains some particles with only three or even two molecules of apoA-I per particle. Supplementary Table 1 shows the number of molecules of each major component of the particles studied, based on these calculations. It should be noted that our previous estimates of apoA-I molecules per particle in native HDL particles were slightly lower and range from 2.9 in HDL_{3c} to 4.3 in HDL_{2b} (ref. 29), likely owing to the removal of apoA-I-poorer LpA-I:A-II particles by covalent chromatography.

We also analyzed the contributions of lipid and protein to the total surface area of the particles. Using data from surface balance experiments on HDL lipids indicating molecular surface areas of 65 Å² per phospholipid molecule³⁰ and 40 Å² per cholesterol³⁰, we found that total surface lipids accounted for only 33, 26, 23, 18 and 12% of the total surface area of LpA-I_{2b} through LpA-I_{3c}, respectively. They accounted for even less area when values from molecular dynamics simulations were assumed (27, 21, 19, 15 and 10%, respectively, based on 55 Å² for phospholipid and 27 Å² for cholesterol³¹); thus, by any measure, the outer shell of these particles is dominated by apoA-I.

Cross-linking and mass spectrometry

Each subfraction was cross-linked, delipidated, subjected to exhaustive trypsin digestion and then analyzed by ESI-MS. Table 2 summarizes all MS/MS-verifiable cross-links found in three separate experiments (see Online Methods). We identified 39 cross-links among the five subfractions. Of these, 25 had been identified in our previous studies of both discoidal and spherical reconstituted HDL particles. In addition, we identified a set of 14 cross-links that were not found in reconstituted HDL particles. Unexpectedly, most cross-links

were distributed equally across the five subfractions, indicating that apoA-I contacts do not vary substantially among them, despite differences in particle diameter.

Because the gel-filtration analysis (Fig. 1b) showed considerable size overlap among the LpA-I species, even between LpA-I_{2b} and LpA-I_{3c}, we were concerned that the similarity in cross-linking patterns may have occurred because of particle cross-contamination. To test this, we isolated LpA-I_{2b} and LpA-I_{3b} fractions by ultracentrifugation and disulfide chromatography as described above and then subjected the fractions to high-resolution gel-filtration chromatography using three Superdex 200 columns connected in series³². LpA-I_{3b} was selected rather than LpA-I_{3c} to avoid albumin contamination (Fig. 1). We then isolated the largest fractions of LpA-I_{2b} and the smallest fractions of LpA-I_{3b}. The native PAGE analysis of these fractions indicated no size overlap between the samples (Supplementary Fig. 5a). Cross-linking of both samples again showed a nearly identical pattern consistent with the data in Table 2 (Supplementary Fig. 5b). Therefore, our data strongly indicate that apoA-I molecular contacts do not vary substantially between the smallest, densest HDL particles and the largest, lightest HDL particles in human plasma.

ApoA-I conformation in LpA-I particles

We next evaluated apoA-I structure in the subfractions by three independent methods. First, we used circular dichroism (CD) spectroscopy. Ordinarily, one would not attempt this on physiologically isolated HDL particles because the presence of diverse apolipoproteins would provide only an averaged readout. However, given the dominance of apoA-I in these separated particles (Fig. 1), we reasoned that CD spectroscopy should provide a suitable estimate of its secondary structure. The CD spectral shapes (Fig. 3a) were indicative of highly helical proteins with characteristic minima at 208 nm and 222 nm. LpA-I_{2b} showed a helical content of 76%, consistent with measurements of reconstituted particles²¹. LpA-I_{2b} through LpA-I_{3a} showed no difference in spectral shape, indicating similar secondary structures. However, LpA-I_{3b} and LpA-I_{3c} showed reduced helical content, suggesting that certain apoA-I helical domains are unfolded in the smaller particles. We also evaluated the particles by examining their susceptibility to limited proteolysis

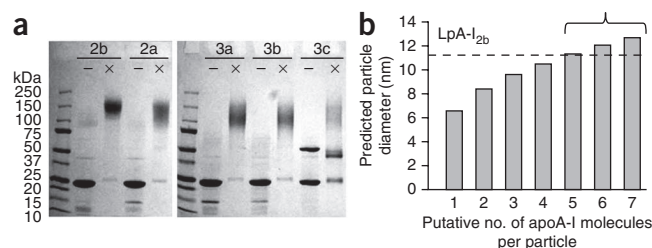


Figure 2 Estimation of the number of apoA-I molecules per particle in LpA-I subfractions. (a) A 4–15% SDS-PAGE analysis of unmodified (–) and cross-linked (x) LpA-I subfractions. The gel was stained with Coomassie blue. (b) Predicted diameters for the LpA-I_{2b} particle given the experimentally derived particle compositions calculated at various numbers of apoA-I molecules per particle (see text). The dashed line shows the experimental particle diameter (averaged from gel filtration and native PAGE, Table 1) for this particle. The bracket indicates the range of possible apoA-I molecules per particle determined by SDS-PAGE analysis of cross-linked LpA-I_{2b} particles (for example, lane 3 in panel a).

Table 2 BS³ cross-links detected in human plasma LpA-I density subclasses

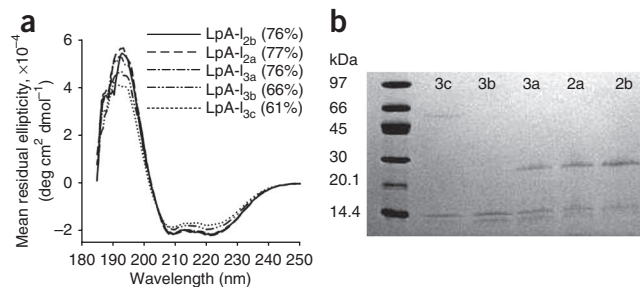
X-link	Th. mass (Da)	Exp. mass (Da)	LpA-I subfraction ^a					Consistent 5/5 or 5/2 DB or TF model?
			2b	2a	3a	3b	3c	
Lys239-Lys239 ^b	1,342.745	1,342.793	3	3	3	3	3	Yes
Lys118-Lys239 ^b	1,608.919	1,608.987	3	3	3	3	3	No
Lys94-Lys239 ^b	1,670.908	1,670.975	3	3	3	2	1	No
Lys88-Lys94	1,671.838	1,671.888	3	3	3	3	3	Yes
Lys96-Lys106	1,716.908	1,716.976	2	0	0	0	0	Yes
Lys208-Lys239 ^b	1,751.977	1,752.059	3	3	3	3	3	Yes
Lys182-Lys239	1,897.026	1,897.110	2	3	3	3	3	Yes
Nt-Lys239 ^b	1,965.942	1,965.980	2	2	2	3	2	Yes
Lys12-Lys23	2,015.093	2,015.135	3	3	3	3	3	Yes
Lys238-Lys239	2,108.103	2,108.150	1	3	3	3	3	Yes
Lys118-Lys133	2,158.210	2,158.297	2	3	3	3	3	Yes
Lys208-Lys208	2,161.210	2,161.305	3	3	3	3	3	Yes
Lys96-Lys239 ^b	2,191.152	2,191.220	1	3	1	1	0	No
Nt-Lys118	2,232.117	2,232.198	3	3	3	3	3	Yes ^c
Nt-Lys94	2,294.106	2,294.184	3	3	3	3	3	Yes ^c
Lys94-Lys96	2,302.173	2,302.223	2	2	2	3	3	Yes
Lys133-Lys140	2,302.198	2,302.236	3	3	3	3	3	Yes
Lys182-Lys208 ^b	2,306.259	2,306.342	3	3	3	3	3	No
Lys206-Lys208	2,346.242	2,346.313	3	3	3	3	3	No
Lys107-Lys118	2,417.241	2,417.346	2	2	3	3	3	Yes
Lys133-Lys182 ^b	2,446.317	2,446.425	1	1	0	0	0	No
Lys182-Lys182 ^b	2,451.308	2,451.410	3	3	3	1	0	No
Lys96-Lys118	2,457.326	2,457.356	1	1	1	1	1	Yes
Lys12-Lys94	2,530.414	2,530.461	2	3	3	2	3	Yes ^c
Nt-Nt ^b	2,589.140	2,589.221	3	2	0	0	0	Yes
Lys40-Lys239	2,736.433	2,736.509	3	3	3	3	3	Yes
Nt-Lys106	2,743.312	2,743.389	0	3	3	3	0	Yes ^c
Lys182-Lys238	2,808.490	2,808.587	3	3	2	2	2	Yes
Nt-Lys12	2,825.448	2,825.509	3	3	3	3	3	Yes
Lys226-Lys238	2,863.562	2,863.640	0	1	0	1	1	Yes
Lys118-Lys140	2,914.558	2,914.656	3	3	2	2	2	Yes
Lys88-Lys96	2,923.452	2,923.545	3	3	3	3	3	Yes
Lys59-Lys208	3,030.602	3,030.688	2	0	0	0	0	Yes
Nt-Lys40 ^b	3,359.630	3,359.730	2	1	0	0	0	Yes
Lys23-Lys59 ^b	3,668.893	3,669.006	2	3	2	2	2	Yes
Lys40-Lys45	3,727.861	3,727.949	0	0	1	1	0	Yes
Lys182-Lys226 ^b	3,892.087	3,892.191	3	3	3	3	3	Yes
Nt-Lys77 ^b	3,980.870	3,980.970	2	2	2	2	2	Yes ^c
Lys77-Lys195	4,782.366	4,782.496	2	3	2	2	2	Yes

^aThe number of times that an MS/MS-verifiable spectrum was observed in a total of three experiments ($n = 3$). DB, double belt; TF, trefoil. ^bThese cross-links are unique to native human plasma LpA-I particles (compared to both discoidal and spherical reconstituted particles). ^cThese cross-links are consistent with the N terminus doubling back on the belt in the double-belt model^{6,11}.

(Fig. 3b). ApoA-I molecules on LpA-I_{2b}, LpA-I_{2a} and LpA-I_{3a} were relatively resistant to trypsin under these conditions but were substantially more susceptible in the two densest fractions. Finally, we measured the binding of a monoclonal antibody (A-115) that is specific for the central domain of apoA-I (residues 115–126)³³. The association of this antibody was minimal in the HDL_{2b} through HDL_{3a} particles but increased dramatically in HDL_{3c} and trended upwards in HDL_{3b} (Supplementary Fig. 6). Taken together, the CD, proteolysis and antibody-binding studies indicate that apoA-I conformation is similar in the LpA-I_{2b}, LpA-I_{2a} and LpA-I_{3a} particles, but localized conformational differences likely exist in LpA-I_{3b} and LpA-I_{3c}.

Figure 3 Investigating apoA-I conformation in LpA-I particles.

(a) Far UV circular dichroism spectra for the indicated LpA-I subfractions. The inset shows the calculated percent helicity of apoA-I with a typical s.d. of $\pm 5\%$. (b) An 8–25% SDS-PAGE analysis of LpA-I subfractions subjected to limited trypsin digestion and stained with Coomassie blue. Both panels show representative results from two independent experiments.

**Evaluation of the trefoil model in LpA-I**

We next determined the plausibility of all cross-links in Table 2 with respect to the trefoil model of apoA-I in spherical HDL²¹ (see introduction). Of the 39 identified cross-links, 32 were judged to be consistent with the 5/5 (or 5/2) forms of the double-belt trefoil models; in other words, the side chain amine groups of the involved lysines could be within the 11.4 Å spacer arm of the cross-linker¹⁰. These include the critical long-range cross-links such as Lys118-Lys140, Lys59-Lys208 and Lys77-Lys195 that distinguish the antiparallel belt model⁸. The 5/5 trefoil model is shown in Figure 4 with applicable cross-links from Table 2 shown in red, illustrating the concordance of the model with the data.

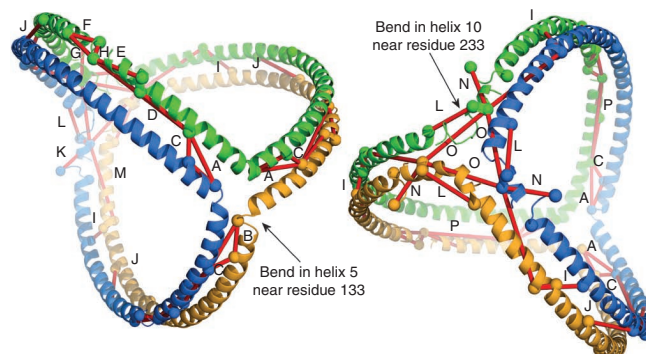
To further refine how the base trefoil model might apply to the different-sized LpA-I species, we began by considering the largest particle, LpA-I_{2b}. In its fully extended form, the trefoil model defines a spherical particle with a diameter of about 10.8 nm, reasonably close to the experimentally determined diameter of LpA-I_{2b} of 11.2 nm. However, LpA-I_{2b} contains, on average, five apoA-I molecules versus three in the trefoil. This discrepancy can be resolved by intercalating two additional apoA-I molecules with a corresponding decrease in the apoA-I bend angles so that each creates a 72° biangle versus 120° for the trefoil (Fig. 5a,b). This ‘pentafoil’ markedly increases the percentage of the particle surface area occupied by protein, but the particle diameter remains consistent with LpA-I_{2b}. Notably, all apoA-I molecules make similar intermolecular contacts, consistent with the cross-linking data. The original trefoil model was built without the N-terminal 43 amino acids of apoA-I; thus, the diameter predicted by the trefoil is likely smaller than that generated by full-length apoA-I and this

may account for the small difference in size between the trefoil prediction and the measured LpA-I_{2b} diameter. We also point out that models related to the double belt such as the ‘belt and buckle’ model (in which the N terminus lays back across the belts)⁷ is consistent with this arrangement. Indeed, several of the cross-links in Table 2 (see footnotes) support this idea.

In the case of LpA-I_{2a}, only one molecule needs to be added to the trefoil. However, the predicted diameter of 10.8 nm is larger than

Figure 4 Trefoil model of apoA-I on spherical particles with experimental cross-links derived from human plasma HDL particles. The model contains three apoA-I molecules (modeled with residues 40–243) shown as ribbons, each in a different color. For clarity, no lipids are shown. The same model is shown from two views: (left) looking from the intersection of helix 5 (residue 133) in each molecule and (right) looking down from helix 10 (residue 233).

Cross-links derived from physiological HDL in **Table 2** judged to fit the 5/5 form of the double-belt/trefoil model (see text) are shown as red lines connecting the α -carbons of the involved lysine residues (shown as spheres). Lysines were considered plausible if the α -carbons were within 25 Å (11.4 Å for BS³ and 6.8 Å for each lysine side chain). Clearly visible cross-links are labeled with a letter and refer to: (A) 133–118, (B) 133–140, (C) 140–118, (D) 107–118, (E) 96–106, (F) 88–94, (G) 88–96, (H) 94–96, (I) 208–59, (J) 195–77, (K) 40–239, (L) 226–239, (M) 239–208, (N) 40–239, (O) 239–239 and (P) 96–118. Additional molecules of apoA-I can be added to the trefoil as illustrated in **Figure 5** without affecting the cross-linking patterns, but they are not shown for clarity.



the experimentally measured 9.8 nm (**Fig. 5c**). We can envision two general ways in which the smaller diameter can be accommodated. First, regions of the resident apoA-I molecules could fold off the particle surface to form a hinge domain that reduces the distance between the particle poles^{34,35}. However, one expects that these exposed sites should be hypersensitive to proteolysis. Because the experiments showed no remarkable differences in proteolytic sensitivity or secondary structure between LpA-I_{2b} and LpA-I_{2a} (or LpA-I_{3a}) (**Fig. 3**), we favor a second explanation for varying particle size that involves the twisting of apoA-I molecules on the particle surface (**Fig. 5d**). One can imagine turning the poles of the particle in opposite directions by an angle Θ , shrinking the particle diameter. Using a mathematical modeling program, we calculated the degree of twist required to account for the diameters of LpA-I_{2a} through LpA-I_{3c} (**Fig. 6**). By inducing moderate degrees of twist, we could easily account for the observed experimental diameters of all LpA-I particles, while maintaining the required number of apoA-I molecules. This predicts that the LpA-I_{3c} particle surface is composed almost entirely of protein, with only room enough for a small amount of surface lipids in each biangle, consistent with the relative contributions of protein and phospholipid surface areas measured experimentally. Importantly, this twisting should not result in major changes in the intermolecular registry of apoA-I molecules, consistent with the similarities in cross-linking patterns among the LpA-I species.

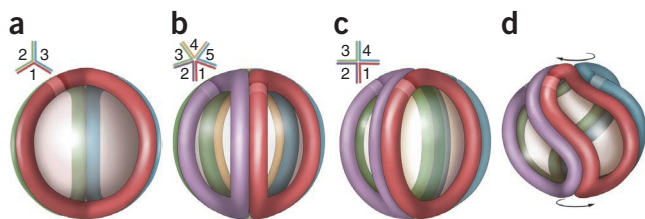


Figure 5 Incorporation of additional apoA-I molecules to the trefoil model and apoA-I adaptation to smaller particle diameters. (a) Schematic representation of the three-molecule trefoil model as originally proposed, with each molecule of apoA-I shown in a different color (see **Fig. 4** for more detail). The lighter color band on each molecule represents the N terminus (residue 44, as the model was built in the absence of residues 1–43). The inset is a schematic top view showing the bend angles of each apoA-I. (b) Pentameric complex proposed for the structure of LpA-I_{2b}. (c) An idealized, fully extended tetrameric complex. (d) Twisted tetrameric complex with a reduced particle diameter as proposed for LpA-I_{2a}.

DISCUSSION

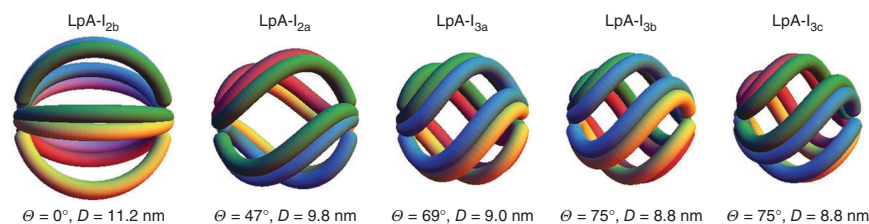
Our laboratory has taken advantage of chemical cross-linking and mass spectrometry to derive distance constraints for apoA-I molecules in HDL with both discoidal and spherical shapes of various sizes prepared *in vitro*. In each case, our data supported the molecular contacts proposed for the double-belt model¹⁰ in particles that have two molecules of apoA-I and the related trefoil model²¹ for those with three. In addition, we interpreted a smaller subset of cross-links to be indicative of an alternative 5/2 registry¹⁰. As little is known about apoA-I structure in plasma-derived HDL particles and as high-resolution structural techniques such as NMR and X-ray crystallography will likely never be applicable to these particles, we extended this methodology to authentic LpA-I HDL. We found that the majority of the cross-links identified in reconstituted particles were also present in plasma-derived particles. Thus, one important finding of this study is that apoA-I adopts a common general structural organization, characterized by distinct intermolecular contacts, in virtually all lipid-containing particles, regardless of size and shape or natural versus synthetic method of production. However, it is also clear that apoA-I can undergo conformational changes within this framework, particularly in the smaller particles (**Fig. 3** and **Supplementary Fig. 6**).

Given the dominance of apoA-I in human HDL, particularly after its enrichment in LpA-I, these data allow us to evaluate models for apoA-I organization in human plasma HDL. In our view, a successful model must account for the following: (i) the presence of multiple apoA-I molecules, both even and odd numbers, on a given particle, (ii) the ability to adapt to different HDL particle diameters and (iii) pursuant to our cross-linking data, the ability to maintain similar intermolecular contacts in all cases. We proposed the modified forms of the trefoil model described above that fit these criteria (**Figs. 5** and **6**), and now discuss its strengths and weaknesses.

An important feature of the trefoil model that allows for intercalation of additional apoA-I molecules is the clamshell-like bending motion at two points, one near residue 133 and the other near 233 (**Fig. 4**). There is ample experimental¹² and theoretical evidence³⁶ for a hinge-like action of the sequence surrounding residue 133 in helix 5. Although less information exists on the flexibility of the region near residue 233 in helix 10, this site is known to be susceptible to V8 protease digestion in reconstituted HDL particles³⁷, potentially consistent with a hinge. However, more work will be required to conclusively demonstrate that this motion occurs at these sites.

The concept of apoA-I molecular twisting to modulate particle size has been proposed previously in discoidal particles^{22,23}. In molecular dynamics simulations, as phospholipids were incrementally removed

Figure 6 Molecular twist required to attain the experimentally LpA-I particle diameters. The helical domains of apoA-I molecules are represented as tubes extending across the particle surface with each molecule in a different color. In LpA-I_{2b}, apoA-I helical domains from five molecules are all maximally extended. The smaller particles contain four apoA-I molecules per particle and each pole has been twisted by an angle θ such that the complex diameter (D) matches the experimentally determined values (average of the diameter values from gel filtration and native PAGE in **Table 1**).



from discoidal particles, they adopted a twisted, saddle shape. Both associated apoA-I molecules also twisted, but they remained attached to the lipids. More recent studies have applied atomistic and coarse-grained simulation methods to simple spherical particles containing a cholesteryl oleate core and two molecules of apoA-I³⁸. These also demonstrated the potential for apoA-I molecules to twist around the surface of a sphere while still maintaining intermolecular contacts consistent with the double belt. Furthermore, the Borhani crystal structure depicted four apoA-I molecules (PDB: 2A01) that twisted around each other in the absence of lipid³⁹. When amino acids 40–243 of apoA-I were plotted as a single idealized helix, the hydrophobic face made a 360° turn around the helical axis⁵. Given that the hydrophobic face interacts with a fixed lipid surface, it is quite reasonable that the entire molecule twists around a sphere.

A double-superhelix model (DSH) of apoA-I was recently proposed (PDB: 3K2S) in reconstituted particles in which two antiparallel apoA-I molecules, making similar intermolecular contacts as the double belt, form an elongated micellar arrangement instead of a bilayer disc¹⁴. Although this model can be adapted to a spherical surface (see **Supplementary Fig. 7** for a possibility), we favor the trefoil-based model for human plasma LpA-I particles because it allows for both even and odd numbers of apoA-I molecules that all adopt the same conformation. It is not clear how the DSH model can accommodate odd numbers of apoA-I molecules without splitting the superhelix or adding a molecule in a different conformation. In addition, **Table 2** clearly shows N terminus to N terminus as well as C terminus to C terminus cross-links in native LpA-I particles that are predicted in the closed trefoil but not the DSH.

One limitation of the analysis described here is that we were unable to distinguish between intermolecular and intramolecular apoA-I cross-links in the native HDL samples. In our previous work with simple reconstituted particles, we made this distinction by isolating monomeric and dimeric apoA-I from cross-linked particles and analyzing them separately¹⁰. This allowed us to rule out certain hairpin arrangements in favor of the antiparallel double belt in the rHDL particles. Unfortunately, this approach became prohibitively complex in particles containing three or more molecules of apoA-I. Our extrapolations between the double-belt and the trefoil-based models here thus rely on the assumption that cross-links identified as intermolecular in the reconstituted particles are also intermolecular in authentic LpA-I particles. However, we recognize the possibility that hairpins or certain combinations of belts and hairpins could exist in the LpA-I particles in arrangements consistent with our cross-linking data. Nevertheless, considering that the extent of multimer formation as a function of cross-linking reagent concentration is identical between reconstituted discs and LpA-I particles of various size (**Supplementary Fig. 3**), we believe it is unlikely that there are substantial differences between apoA-I contacts on rHDL discs versus LpA-I particles. One would expect this relationship to be quite different if the discs adopted the double belt and the LpA-I particles adopted alternate arrangements

such as hairpins because the degree of intermolecular contact varies dramatically between the two models.

We found seven cross-links that are not predicted by the trefoil-based models (**Table 2**). These exclusively involved residues 182 and 239. The nature of these cross-links is unclear at this point, but they may reflect alternate apoA-I conformations within native HDL particles. Indeed, recent studies⁴⁰ have demonstrated that apoA-I can adopt a distinct conformation on HDL particles that may represent a partially associated transition state. It is also possible that new conformations of apoA-I can be induced by the presence of non-apoA-II proteins on some of the particles. We also acknowledge the possibility that we haven't yet thought of a comprehensive model that explains all the cross-linking data, if one exists.

Implications of the new models for HDL functionality

The models shown in **Figure 6** clearly lack enough resolution to allow speculation of how apoA-I mediates interactions with other proteins. However, our demonstration that apoA-I overwhelmingly dominates the surface of these HDL particles may provide clues to how other HDL-associated proteins interact with these particles. HDL has been shown to contain some 35–50 minor proteins in addition to apoA-I and apoA-II⁴¹, and we recently showed that a majority of these are associated with the smallest²⁸ or most dense HDL_{3c} fractions²⁷. The presumption has been that these proteins associate with the phospholipid surface to coexist with apoA-I. However, it is clear from the models (**Fig. 6**) and our composition calculations that about 85% of the LpA-I_{3c} particle surface is covered by apoA-I. It is thus difficult to imagine how other proteins can find room to bind. One implication of this is that additional proteins may associate directly with apoA-I and not the lipid surface, or they may form their own separate particles that happen to co-fractionate in this density range.

Finally, our limited proteolysis, CD and antibody-binding data indicate that although all subfractions show a similar global structure, the smaller, denser particles have localized structural differences versus the larger, lighter ones. Under high degrees of apoA-I twist, localized areas of apoA-I may unfold without necessarily leaving the particle surface. This concept can be likened to twisting a rubber band until local areas begin to distend. A similar idea was previously proposed in discoidal particles studied by molecular dynamics simulated annealing²³. It was hypothesized that two localized regions, one near the N terminus and the other in helix 8 of apoA-I, lose helicity when discs transition between the planar and saddle-shape morphologies. Our data suggest that a similar transition may occur in physiological spherical particles at the LpA-I_{3a} and LpA-I_{3b} boundary. Whether these conformational changes occur at the same locations in physiological spherical HDL and how they might affect HDL metabolism awaits further study.

In summary, we have provided the most comprehensive set of distance constraints for native human plasma HDL particles achieved to date. The results unambiguously show that apoA-I contacts found in model reconstituted particles occur in authentic human plasma HDL

particles. We extended models originally derived in reconstituted particles to these native species. Our favored scheme, based on our proposed trefoil arrangement, is a parsimonious solution that is consistent with the majority of experimental, geometric and molecular simulation data from this study and others, in which changes in the particle-neutral lipid core are mediated by twisting motions of the surface apoA-I molecules. It remains to be seen how these changes affect important physiological interactions with plasma lipid-remodeling enzymes and cell-surface receptors responsible for HDL metabolism and function.

METHODS

Methods and any associated references are available in the online version of the paper at <http://www.nature.com/nsmb/>.

Accession codes. Protein Model Database: Silva trefoil model of apoA-I(Δ 1-43) in a spherical rHDL particle (hypothesized structure)²¹ is deposited under accession number PM0075240.

Note: Supplementary information is available on the Nature Structural & Molecular Biology website.

ACKNOWLEDGMENTS

This work was supported by US National Institutes of Health (NIH) 01 grant HL67093 (to W.S.D.), an American Heart Association Great Rivers Postdoctoral Fellowship to R.H. (3880030), NIH R01 grant HL48148 (to W.G.J.) and NIH Pathway to Independence Award (K99/R00) HL087561 from the National Heart, Lung, and Blood Institute (to R.A.G.D.S.). Negative stain EM was carried out in the Vanderbilt University Research Electron Microscopy Resource of the Cell Imaging Core. This resource is partially supported by NIH grants CA68485, DK20593 and DK58404. A.K. was supported by Institut National de la Santé et de la Recherche Médicale, Fondation pour la Recherche Médicale en France. The images in **Figure 6** were rendered by M. Hartsock (marcia@hartsockillustration.com). Any use of these images is subject to copyright law and should be negotiated with the artist. We also thank C. Smith for excellent administrative assistance.

AUTHOR CONTRIBUTIONS

R.H., M.J.C. and W.S.D. designed the research plan. R.H., R.A.G.D.S., L.K.C., W.G.J. and A.K. conducted experiments. R.H., W.S.D. and T.J.H. analyzed data, and R.H. and W.S.D. wrote the manuscript.

COMPETING FINANCIAL INTERESTS

The authors declare no competing financial interests.

Published online at <http://www.nature.com/nsmb/>.

Reprints and permissions information is available online at <http://npg.nature.com/reprintsandpermissions/>.

- Gordon, T., Castelli, W.P., Hjortland, M.C., Kannel, W.B. & Dawber, T.R. High density lipoprotein as a protective factor against coronary heart disease. The Framingham Study. *Am. J. Med.* **62**, 707–714 (1977).
- Rye, K.A., Bursill, C.A., Lambert, G., Tabet, F. & Barter, P.J. The metabolism and anti-atherogenic properties of HDL. *J. Lipid Res.* **50** Suppl, S195–S200 (2009).
- Davidson, W.S. & Thompson, T.B. The structure of apolipoprotein A-I in high density lipoproteins. *J. Biol. Chem.* **282**, 22249–22253 (2007).
- Thomas, M.J., Bhat, S. & Sorci-Thomas, M.G. Three-dimensional models of HDL apoA-I: implications for its assembly and function. *J. Lipid Res.* **49**, 1875–1883 (2008).
- Segrest, J.P., Harvey, S.C. & Zannis, V. Detailed molecular model of apolipoprotein A-I on the surface of high-density lipoproteins and its functional implications. *Trends Cardiovasc. Med.* **10**, 246–252 (2000).
- Koppaka, V., Silvestro, L., Engler, J.A., Brouillette, C.G. & Axelsen, P.H. The structure of human lipoprotein A-I. Evidence for the 'belt' model. *J. Biol. Chem.* **274**, 14541–14544 (1999).
- Bhat, S., Sorci-Thomas, M.G., Alexander, E.T., Samuel, M.P. & Thomas, M.J. Intermolecular contact between globular N-terminal fold and C-terminal domain of ApoA-I stabilizes its lipid-bound conformation: studies employing chemical cross-linking and mass spectrometry. *J. Biol. Chem.* **280**, 33015–33025 (2005).
- Davidson, W.S. & Hilliard, G.M. The spatial organization of apolipoprotein A-I on the edge of discoidal high density lipoprotein particles: A mass spectrometry study. *J. Biol. Chem.* **278**, 27199–27207 (2003).
- Panagotopoulos, S.E., Horace, E.M., Maiorano, J.N. & Davidson, W.S. Apolipoprotein A-I adopts a belt-like orientation in reconstituted high density lipoproteins. *J. Biol. Chem.* **276**, 42965–42970 (2001).
- Silva, R.A., Hilliard, G.M., Li, L., Segrest, J.P. & Davidson, W.S. A mass spectrometric determination of the conformation of dimeric apolipoprotein A-I in discoidal high density lipoproteins. *Biochemistry* **44**, 8600–8607 (2005).
- Bhat, S., Sorci-Thomas, M.G., Tuladhar, R., Samuel, M.P. & Thomas, M.J. Conformational adaptation of apolipoprotein A-I to discretely sized phospholipid complexes. *Biochemistry* **46**, 7811–7821 (2007).
- Martin, D.D., Budamagunta, M.S., Ryan, R.O., Voss, J.C. & Oda, M.N. Apolipoprotein A-I assumes a 'looped belt' conformation on reconstituted high density lipoprotein. *J. Biol. Chem.* **281**, 20418–20426 (2006).
- Wu, Z. *et al.* The refined structure of nascent HDL reveals a key functional domain for particle maturation and dysfunction. *Nat. Struct. Mol. Biol.* **14**, 861–868 (2007).
- Wu, Z. *et al.* Double superhelix model of high density lipoprotein. *J. Biol. Chem.* **284**, 36605–36619 (2009).
- Gogonea, V. *et al.* Congruency between biophysical data from multiple platforms and molecular dynamics simulation of the double-super helix model of nascent high-density lipoprotein. *Biochemistry* **49**, 7323–7343 (2010).
- Jones, M.K. *et al.* Assessment of the validity of the double superhelix model for reconstituted high density lipoproteins: a combined computational-experimental approach. *J. Biol. Chem.* **285**, 41161–41171 (2010).
- Jonas, A., Wald, J.H., Toohill, K.L., Krul, E.S. & Kezdy, K.E. Apolipoprotein A-I structure and lipid properties in homogeneous, reconstituted spherical and discoidal high density lipoproteins. *J. Biol. Chem.* **265**, 22123–22129 (1990).
- Segrest, J.P., Garber, D.W., Brouillette, C.G., Harvey, S.C. & Anantharamaiah, G.M. The amphipathic alpha helix: a multifunctional structural motif in plasma apolipoproteins. *Adv. Protein Chem.* **45**, 303–369 (1994).
- Li, H.H. *et al.* ApoA-I structure on discs and spheres. Variable helix registry and conformational states. *J. Biol. Chem.* **277**, 39093–39101 (2002).
- Sparks, D.L., Phillips, M.C. & Lund-Katz, S. The conformation of apolipoprotein A-I in discoidal and spherical recombinant high density lipoprotein particles. ¹³C NMR studies of lysine ionization behavior. *J. Biol. Chem.* **267**, 25830–25838 (1992).
- Silva, R.A. *et al.* Structure of apolipoprotein A-I in spherical high density lipoproteins of different sizes. *Proc. Natl. Acad. Sci. USA* **105**, 12176–12181 (2008).
- Catte, A. *et al.* Novel changes in discoidal high density lipoprotein morphology: a molecular dynamics study. *Biophys. J.* **90**, 4345–4360 (2006).
- Gu, F. *et al.* Structures of discoidal high density lipoproteins: a combined computational-experimental approach. *J. Biol. Chem.* **285**, 4652–4665 (2010).
- Kontush, A., Chantepie, S. & Chapman, M.J. Small, dense HDL particles exert potent protection of atherogenic LDL against oxidative stress. *Arterioscler. Thromb. Vasc. Biol.* **23**, 1881–1888 (2003).
- Rosales, C., Gillard, B.K., Courtney, H.S., Blanco-Vaca, F. & Pownall, H.J. Apolipoprotein modulation of streptococcal serum opacity factor activity against human plasma high-density lipoproteins. *Biochemistry* **48**, 8070–8076 (2009).
- Kontush, A. *et al.* Preferential sphingosine-1-phosphate enrichment and sphingomyelin depletion are key features of small dense HDL3 particles: relevance to antiapoptotic and antioxidative activities. *Arterioscler. Thromb. Vasc. Biol.* **27**, 1843–1849 (2007).
- Davidson, W.S. *et al.* Proteomic analysis of defined HDL subpopulations reveals particle-specific protein clusters: relevance to antioxidative function. *Arterioscler. Thromb. Vasc. Biol.* **29**, 870–876 (2009).
- Brouillette, C.G. & Anantharamaiah, G.M. Structural models of human apolipoprotein A-I. *Biochim. Biophys. Acta* **1256**, 103–129 (1995).
- de Souza, J.A. *et al.* Metabolic syndrome features small, apolipoprotein A-I-poor, triglyceride-rich HDL3 particles with defective anti-apoptotic activity. *Atherosclerosis* **197**, 84–94 (2008).
- Ibdah, J.A., Lund-Katz, S. & Phillips, M.C. Molecular packing of high-density and low-density lipoprotein surface lipids and apolipoprotein A-I binding. *Biochemistry* **28**, 1126–1133 (1989).
- Hofsäss, C., Lindahl, E. & Edholm, O. Molecular dynamics simulations of phospholipid bilayers with cholesterol. *Biophys. J.* **84**, 2192–2206 (2003).
- Gordon, S.M., Deng, J., Lu, L.J. & Davidson, W.S. Proteomic characterization of human plasma high density lipoprotein fractionated by gel filtration chromatography. *J. Proteome Res.* **9**, 5239–5249 (2010).
- Curtiss, L.K., Bonnet, D.J. & Rye, K.A. The conformation of apolipoprotein A-I in high-density lipoproteins is influenced by core lipid composition and particle size: a surface plasmon resonance study. *Biochemistry* **39**, 5712–5721 (2000).
- Córsico, B., Toledo, J.D. & Garda, H.A. Evidence for a central apolipoprotein A-I domain loosely bound to lipids in discoidal lipoproteins that is capable of penetrating the bilayer of phospholipid vesicles. *J. Biol. Chem.* **276**, 16978–16985 (2001).
- Maiorano, J.N., Jandacek, R.J., Horace, E.M. & Davidson, W.S. Identification and structural ramifications of a hinge domain in apolipoprotein A-I discoidal high-density lipoproteins of different size. *Biochemistry* **43**, 11717–11726 (2004).
- Jones, M.K., Catte, A., Li, L. & Segrest, J.P. Dynamics of activation of lecithin: cholesterol acyltransferase by apolipoprotein A-I. *Biochemistry* **48**, 11196–11210 (2009).
- Roberts, L.M. *et al.* Structural analysis of apolipoprotein A-I: limited proteolysis of methionine-reduced and -oxidized lipid-free and lipid-bound human apo A-I. *Biochemistry* **36**, 7615–7624 (1997).
- Catte, A. *et al.* Structure of spheroidal HDL particles revealed by combined atomistic and coarse-grained simulations. *Biophys. J.* **94**, 2306–2319 (2008).
- Borhani, D.W., Rogers, D.P., Engler, J.A. & Brouillette, C.G. Crystal structure of truncated human apolipoprotein A-I suggests a lipid-bound conformation. *Proc. Natl. Acad. Sci. USA* **94**, 12291–12296 (1997).
- Lund-Katz, S. *et al.* Surface plasmon resonance analysis of the mechanism of binding of apoA-I to high density lipoprotein particles. *J. Lipid Res.* **51**, 606–617 (2010).
- Vaisar, T. *et al.* Shotgun proteomics implicates protease inhibition and complement activation in the antiinflammatory properties of HDL. *J. Clin. Invest.* **117**, 746–756 (2007).

ONLINE METHODS

HDL subfractionation and LpA-I isolation. Normolipidemic human EDTA plasma was subjected to a one-step gradient density ultracentrifugation procedure⁴². Lipoprotein fractions (VLDL, LDL and HDL) of 0.8 ml each were collected from top to bottom of the tube and the fractions corresponding to the five HDL subclasses²⁶: HDL_{2b} (density, 1.063 to 1.090 g ml⁻¹), HDL_{2a} (density, 1.090 to 1.120 g ml⁻¹), HDL_{3a} (density, 1.120 to 1.150 g ml⁻¹), HDL_{3b} (density, 1.150 to 1.180 g ml⁻¹) and HDL_{3c} (density, 1.180 to 1.210 g ml⁻¹) from multiple centrifuge tubes were pooled, concentrated by ultrafiltration and dialyzed into standard Tris buffer (STB) for further LpA-I HDL isolation. These density ranges were slightly different from previous reports⁴³ and likely represent slight intralab variations between the French and US laboratories. Three individual human plasma preparations were used for the study ($n = 3$).

To isolate LpA-I from LpA-I–A-II HDL density subfractions, we used the sulfhydryl covalent chromatography technique²⁵ with modifications (details are in **Supplementary Methods**).

Particle composition and characterization. The protein was determined by Markwell-modified Lowry assay⁴⁴, the phospholipid, total cholesterol, free cholesterol and triglyceride contents were determined using enzymatic assay kits from Wako Diagnostics. Cholesteryl ester concentrations were calculated by subtraction of free cholesterol concentrations from total cholesterol concentration and then multiplied by 1.67 (molecular weight of cholesteryl ester divided by molecular weight of free cholesterol). Particle size distribution was assessed by gel filtration using a calibrated Superdex 200 column (GE Healthcare). Particle Stokes diameters were measured on cross-linked particles by native PAGE (Phast system, GE Healthcare). Negative stain EM (**Supplementary Methods**) was also done on LpA-I subfractions as an independent approach to assess particle sizes.

Circular dichroism, limited proteolysis and surface plasmon resonance with monoclonal antibody experiments are described in **Supplementary Methods**.

Secondary structure estimations in **Figure 3** were performed using the SELCON3 algorithm (<http://lamar.colostate.edu/~sreeram/SELCON3/>), hosted at Colorado State University. **Figure 5** was rendered using Adobe Photoshop and **Figure 7** was rendered using Mathematica 7 (Wolfram Research).

Cross-linking and mass spectrometry measurements and data analysis. LpA-I subfractions (1 mg ml⁻¹) dialyzed into PBS were cross-linked with a homo-functional cross-linker, bis(sulfosuccinimidyl) suberate (BS³) (Thermo Scientific) at a protein to BS³ molar ratio of 1:50 that was optimized for the maximum formation of the high-order oligomers (**Supplementary Fig. 3**). We carried out the cross-linking reaction, chloroform-methanol delipidation and trypsin digestion for MS analysis using our optimized protocols (**Supplementary Methods**).

MS measurements of cross-linked particles were taken on a Sciex/Applied Biosystems QSTAR XL coupled with an Agilent on-line capillary HPLC (**Supplementary Methods**). The MS data analysis was carried out using the

Mascot Script in the instrument software and home-built software using our previously described criteria for cross-links (**Supplementary Methods**).

Building the twisted particle models. The models in **Figure 6** were produced using the Mathematica 7 software package. In each case, the apoA-I proteins are represented by a pair of like-colored tubes lying on the surface of a sphere. The leftmost panel shows five molecules of apoA-I lying in a symmetric pentafoil arrangement on the LpA-I_{2b} particle. The molecules have bend angles slightly less than 72° (the reduction being necessary to enable separation of the molecules from each other). The remaining panels represent twisted quatrefoil arrangements of four apoA-I molecules on the LpA-I_{2a}, LpA-I_{3a}, LpA-I_{3b} and LpA-I_{3c} particles. The strands have been twisted in such a way that the twist at the poles is $\pm\Theta$ and the intermediary twisting is a linear function of distance along the polar axis; thus, for instance, the axis of one strand is given by the vector function

$$r(u) = \left[R \cos u, R \sin u \cos(\Theta \cos[u]), R \sin u \sin(\Theta \cos[u]) \right] \quad (1)$$

The path of the axes of the remaining strands is obtained by rotating this curve around the polar axis. The twist Θ is determined by requiring that the strands retain a constant length. The length of such a strand as a function of the twist angle is given by

$$L(\Theta) = R \int_0^\pi \sqrt{1 + \Theta^2 \sin^4 u} \, du \quad (2)$$

In the models, the helical diameter of the apoA-I proteins is assumed to be 11 Å. **Supplementary Table 2** shows the total particle diameter A , the radius R of the sphere on which the axes of the apoA-I helices lie and the twist angle Θ required for the proteins to fit on the particle in this fashion.

Particle volume, diameter and surface area calculations. We calculated the particle volume from the experimentally determined molar ratio of various lipid components and derived the particle diameter from the calculated particle volume. Particle surface-area calculations were taken from compositional data for phospholipids and free cholesterol. Details are described in **Supplementary Methods**.

42. Chapman, M.J., Goldstein, S., Lagrange, D. & Laplaud, P.M. A density gradient ultracentrifugal procedure for the isolation of the major lipoprotein classes from human serum. *J. Lipid Res.* **22**, 339–358 (1981).
43. Zerrad-Saadi, A. *et al.* HDL3-mediated inactivation of LDL-associated phospholipid hydroperoxides is determined by the redox status of apolipoprotein A-I and HDL particle surface lipid rigidity: relevance to inflammation and atherogenesis. *Arterioscler. Thromb. Vasc. Biol.* **29**, 2169–2175 (2009).
44. Markwell, M.A., Haas, S.M., Bieber, L.L. & Tolbert, N.E. A modification of the Lowry procedure to simplify protein determination in membrane and lipoprotein samples. *Anal. Biochem.* **87**, 206–210 (1978).